Check for updates

Analysis of Complement-Mediated Lysis of Simian Immunodeficiency Virus (SIV) and SIV-Infected Cells Reveals Sex Differences in Vaccine-Induced Immune Responses in Rhesus Macaques

Leia K. Miller-Novak,[a]* Jishnu Das,[b] Thomas A. Musich,[a]* Thorsten Demberg,[a]* Joshua A. Weiner,[c] David J. Venzon,[d] Venkatramanan Mohanram,[a] Diego A. Vargas-Inchaustegui,[a] Iskra Tuero,[a]* Margaret E. Ackerman,[c] Galit Alter,[b] Marjorie Robert-Guroff[a]

[a]Vaccine Branch, Center for Cancer Research, National Cancer Institute, National Institutes of Health, Bethesda, Maryland, USA

[b]Ragon Institute of MGH, MIT and Harvard University, Cambridge, Massachusetts, USA

[c]Thayer School of Engineering, Dartmouth College, Hanover, New Hampshire, USA

[d]Biostatistics and Data Management Section, National Cancer Institute, National Institutes of Health, Bethesda, Maryland, USA

ABSTRACT An effective human immunodeficiency virus (HIV) vaccine has yet to be developed, and defining immune correlates of protection against HIV infection is of paramount importance to inform future vaccine design. The complement system is a component of innate immunity that can directly lyse pathogens and shape adaptive immunity. To determine if complement lysis of simian immunodeficiency virus (SIV) and/or SIV-infected cells represents a protective immune correlate against SIV infection, sera from previously vaccinated and challenged rhesus macaques were analyzed for the induction of antibody-dependent complement-mediated lysis (ADCML). Importantly, the vaccine regimen, consisting of a replication-competent adenovirus type 5 host-range mutant SIV recombinant prime followed by a monomeric gp120 or oligomeric gp140 boost, resulted in overall delayed SIV acquisition only in females. Here, sera from all vaccinated animals induced ADCML of SIV and SIV-infected cells efficiently, regardless of sex. A modest correlation of SIV lysis with a reduced infection rate in males but not females, together with a reduced peak viremia in all animals boosted with gp140, suggested a potential for influencing protective efficacy. Gag-specific IgG and gp120-specific IgG and IgM correlated with SIV lysis in females, while Env-specific IgM correlated with SIV-infected cell lysis in males, indicating sex differences in vaccine-induced antibody characteristics and function. In fact, gp120/gp140-specific antibody functional correlates between antibody-dependent cellular cytotoxicity, antibody-dependent phagocytosis, and ADCML as well as the gp120-specific IgG glycan profiles and the corresponding ADCML correlations varied depending on the sex of the vaccinees. Overall, these data suggest that sex influences vaccine-induced antibody function, which should be considered in the design of globally effective HIV vaccines in the future.

IMPORTANCE An HIV vaccine would thwart the spread of HIV infection and save millions of lives. Unfortunately, the immune responses conferring universal protection from HIV infection are poorly defined. The innate immune system, including the complement system, is an evolutionarily conserved, basic means of protection from infection. Complement can prevent infection by directly lysing incoming pathogens. We found that vaccination against SIV in rhesus macaques induces antibodies that are capable of directing complement lysis of SIV and SIV-infected cells in both sexes. We also found sex differences in vaccine-induced antibody species and their func-

Address correspondence to Marjorie Robert-Guroff, guroffm@mail.nih.gov.

* Present address: Leia K. Miller-Novak, Division of Blood Diseases and Resources, National Heart, Lung, and Blood Institute, National Institutes of Health, Bethesda, Maryland, USA; Thomas A. Musich, Department of Retrovirology, AFRIMS, Bangkok, Thailand; Thorsten Demberg, Immatics US Inc., Houston, Texas, USA; Iskra Tuero, Laboratorios de Investigación y Desarrollo, Facultad de Ciencias y Filosofía, Universidad Peruana Cayetano Heredia, Lima, Perú.

tions. Overall, our data suggest that sex affects vaccine-induced antibody characteristics and function and that males and females might require different immune responses to protect against HIV infection. This information could be used to generate highly effective HIV vaccines for both sexes in the future.

KEYWORDS rhesus macaque, SIV vaccine, antibody glycosylation, antibody-dependent complement-mediated lysis, sex bias

According to the most recent global statistics, 2.1 million people became newly infected with human immunodeficiency virus (HIV) in 2015, increasing the number of people currently living with HIV to 36.7 million worldwide (1). The development of an effective vaccine could eradicate the spread of HIV infection, but vaccination efforts have been relatively unsuccessful thus far. This could be attributed, at least in part, to the fact that numerous preclinical/clinical HIV vaccine studies have reported variable, vector-specific efficacies, making it difficult to define universal, vaccine-inducible immune responses that protect from HIV infection. The most successful HIV vaccine to date, evaluated in the RV144 clinical trial (2), demonstrated an overall efficacy of only 31%. In that study, a reduced risk of HIV infection correlated with the following vaccine-induced immune responses: HIV Env V1/V2-specific nonneutralizing IgG, low Env-specific serum IgA, and a polyfunctional Env-specific CD4$^+$ T cell response (3). Whether these correlates of protection are universal and not vaccine platform and/or population specific remains to be determined. Importantly, immune correlate analyses from the RV144 clinical trial highlighted the potential for nonneutralizing antibodies to mediate protection from HIV acquisition (3, 4). Nonneutralizing antibodies have also been implicated in reducing the rates of acquisition of neutralization-resistant simian immunodeficiency virus (SIV) mac251 (SIV$_{mac251}$) (5, 6) and difficult-to-neutralize simian-human immunodeficiency virus (SHIV) SF162P3 (SHIV$_{SF162P3}$) in vaccinated nonhuman primates (7).

In the context of vaccination, a rather underexplored nonneutralizing antibody function is the activation of the complement system. The complement system is composed of several soluble and membrane-bound proteins that participate in innate immunity and augment adaptive immune responses (for reviews, see references 8 and 9). Complement is activated through a series of sequential enzymatic protein cleavage steps. Complement protein cleavage products can (i) opsonize pathogens to enhance phagocytosis, stimulate antigen-presenting cells, boost killing by natural killer cells and granulocytes, enable antigen transport to and retention in secondary lymphoid tissues, and promote B cell activation and germinal center formation (10–12); (ii) act as proinflammatory mediators called anaphylatoxins; and (iii) form the terminal membrane attack complex (MAC) of the complement cascade that functions to directly lyse pathogens by forming lytic pores in their membranes (8, 9, 13). There are three different pathways of complement activation: the classical, lectin, and alternative pathways. The complement recognition protein C1q is responsible for triggering the classical pathway of the complement cascade. C1q can become activated upon its direct recognition of pathogen-associated molecular patterns or upon binding the Fc portion of IgM or IgG antibodies complexed with antigen to induce the cleavage cascade. Mannose-binding lectin (MBL) is the most well-characterized complement recognition protein responsible for triggering the lectin pathway of the complement cascade. MBL recognizes pathogen-specific carbohydrate patterns and induces the cleavage cascade through the activation of MBL-associated serine proteases. The alternative pathway is constitutively activated through a process known as tick-over, which involves the spontaneous hydrolysis of a thioester bond in the complement protein C3. This hydrolysis induces a structural change in C3 allowing it to form an enzymatic complex that is capable of cleaving C3 molecules into C3a and C3b. In fact, all three pathways converge at the cleavage step of C3 to generate C3a and C3b. C3a and the downstream cleavage product C5a act as powerful proinflammatory mediators. C3b opsonizes pathogens by

covalently binding hydroxyl groups on the surface and from there propagates the complement cascade to induce lysis of the pathogen (8, 9).

Not surprisingly, complement deficiencies have been reported to enhance the severity of some bacterial and viral infections, including hepatitis C virus and herpes-virus infections, and to contribute to hepatitis B vaccine failure (13). In the context of HIV infection, MBL deficiency is associated with an increased risk of vertical HIV transmission and HIV disease progression in children less than 2 years old (14). HIV can activate the classical pathway of complement either via an antibody-independent mechanism involving the direct binding of C1q to gp41 (15, 16) or through an antibody-dependent mechanism where C1q binds the Fc portions of HIV-bound IgM and/or IgG antibodies (17, 18). HIV can also activate the lectin pathway through the direct binding of MBL to gp120 (19). Indeed, complement does become activated during HIV infection *in vivo* (20, 21), and antibodies capable of inducing complement-mediated lysis of both autologous and heterologous HIV and HIV-infected cells are readily generated in patients infected with HIV (17, 18, 22–24). In fact, complement-mediated lysis of autologous strains of HIV correlated with lower viral loads in a cohort of 25 patients with acute HIV infection (24). Also, an association between plasma-mediated C3b deposition on HIV gp120-coated target cells and protection of vacci-nated rhesus macaques from infection with $SHIV_{SF162P3}$ was reported (7). In line with that finding, sterilizing immunity to SIV infection in vaccinated cynomolgus macaques was correlated with vaccine-induced HLA-specific antibodies that neutralized SIV in a complement-dependent manner (25). Finally, it was recently reported that HIV Env V1V2-specific IgG-mediated complement activation correlated with a reduced risk of HIV infection in the RV144 trial (26). These studies indicate that nonneutralizing antibodies capable of directing complement-mediated lysis of HIV and/or HIV-infected cells could represent an underappreciated, vaccine-inducible immune correlate of protection against HIV infection.

Recently, we conducted an SIV vaccine study in rhesus macaques in which we observed, for the first time, a sex bias in SIV vaccine efficacy. Vaccinated females exhibited a reduced risk of SIV infection that correlated with mucosal B cell responses (27). Follow-up studies identified additional immune correlates that differed by sex. IgG subclass (IgG1, IgG2, and IgG3) levels were elevated in vaccinated female macaques; IgG3 antibodies, in particular, correlated with antibody-dependent cellular cytotoxicity (ADCC) and antibody-dependent phagocytosis (ADCP) activities and decreased peak viremia in females but not males (28). Env-specific T follicular helper (Tfh) cells were shown to be elevated in vaccinated females and correlated with ADCC activity (29), suggesting a mechanism by which differences in IgG subtype levels might occur. Also, elevated B regulatory (Breg) cell levels were observed in male macaques and directly correlated with peak viremia, suggesting the possible facilitation of SIV infection (28). To identify additional immune correlates of protection to further our understanding of the sex bias, we analyzed vaccine-induced, antibody-dependent complement-mediated lysis (ADCML) of SIV and SIV-infected cells using sera collected from the animals prior to virus challenge. Here, we found that sera collected from all vaccinated animals efficiently induced ADCML of SIV and SIV-infected cells, regardless of sex. Evidence suggesting that ADCML influenced the rate of SIV infection in male macaques led to further studies showing that sex influenced vaccine-induced antibody function-ality, as gp120- and Gag-specific IgG and gp120-specific IgM correlated with SIV lysis only in females, while SIV-infected cell lysis correlated with Env-specific IgM only in males. Moreover, gp120- and gp140-specific antibody functional correlates between ADCC, ADCP, and ADCML as well as antibody glycan profiles and their corresponding correlations with ADCML were different depending on the sex of the vaccinees. These data imply that sex skews vaccine-induced antibody development and subsequent function and suggests that these phenomena should be considered in the design of future HIV vaccines.

RESULTS

Vaccine-induced antibodies mediate ADCML of SIV virions. First, we wanted to assess the role of vaccine-induced complement-mediated immunity in protecting from or helping to control SIV infection. For this, we used sera collected during an SIV vaccine study from rhesus macaques that had been immunized with a prime-boost regimen consisting of two sequential mucosal immunizations with recombinant adenovirus type 5 host-range mutant vectors encoding SIV genes followed by two boosts with either monomeric SIV gp120 or oligomeric SIV gp140 proteins (see Materials and Methods and reference 27 for details). Importantly, vaccinated female animals from that study exhibited delayed SIV acquisition, correlated with Env-specific IgA in rectal secretions and Env-specific memory B cells and total plasma cells in rectal tissue. With those results in mind, we wanted to determine whether complement-mediated activity also represented a sex-biased protective immune correlate. For that purpose, we analyzed ADCML of SIV_{mac251} propagated in primary rhesus macaque peripheral blood mononuclear cells (rPBMCs). To form SIV-antibody immune complexes capable of activating complement, the virus was incubated with heat-inactivated SIV-specific serum from individual rhesus macaques (collected at week 57, 2 weeks before the first viral challenge). Then, autologous non-heat-inactivated serum from each macaque, collected prior to immunization (preimmune complement serum), was added as a source of complement, and SIV lysis was subsequently analyzed via p27 release for all 60 animals from the vaccine study. We observed negligible SIV lysis, on average, in the control samples ($<5\%$; data not shown) that were designed to assess lysis independently of SIV-specific antibodies. Sera from gp140-immunized animals lysed significantly more SIV than sera from gp120-immunized animals ($P < 0.0001$) and mock-vaccinated control animals ($P < 0.0001$), lysing approximately 26% of input virus (Fig. 1A). Sera from gp120-immunized animals also lysed significantly more virus ($\sim$7%) than sera from mock-vaccinated controls (Fig. 1A; $P = 0.0098$). These data are in line with those from our previous report, which indicated that the gp140 protein boost was more immunogenic than the gp120 boost, eliciting, for example, gp140-specific IgG titers higher than those in gp120-immunized animals (27). However, there were no significant sex-specific differences in the percentage of SIV lysed by vaccinated animals' sera; sera from both vaccinated males and females lysed significantly more virus ($\sim$16%) than mock-vaccinated controls (Fig. 1B; $P < 0.02$). Similar results were obtained using heat-inactivated sera collected at week 53, the time of peak antibody activity 2 weeks after the second protein boost (data not shown), although, as expected, the levels of SIV lysis were somewhat higher.

ADCML of SIV depends on complement activation. To confirm that the SIV lysis observed was due to the activation of complement, we performed two experiments. First, equal aliquots of SIV ADCML samples (prepared as indicated above) from three different animals were assessed for complement activation via Western blotting. Upon complement activation, regardless of the activation pathway, component C3 ($\sim$185 kDa) is cleaved into C3a and C3b ($\sim$110 kDa). Therefore, we probed our Western blot using an antibody specific for an epitope in the C-terminal region of the alpha chain of C3 that recognizes both C3 and C3b. Complement activation was readily detectable in the SIV ADCML samples analyzed, as indicated by a decrease in the C3 band density with a concomitant increase in the C3b band density (Fig. 1C, lane 4). Controls for complement activation were included and consisted of autologous heat-inactivated, nonspecific serum (preimmune hiserum) mixed with SIV (Fig. 1C, lane 1) to serve as a negative control and autologous preimmune complement serum treated with cobra venom factor (CVF) (Fig. 1C, lane 2) to serve as a positive control. In comparing the ratio of the C3b to C3 band densities within each lane, significantly more C3 was processed into C3b, indicating more robust complement activation in the samples containing SIV-specific serum than in the samples containing nonspecific serum (Fig. 1C, lane 4 versus lane 3, and D; $P = 0.025$) and also than in the negative-control samples (Fig. 1C, lane 4 versus lane 1, and D; $P = 0.0001$). Background complement activation in the
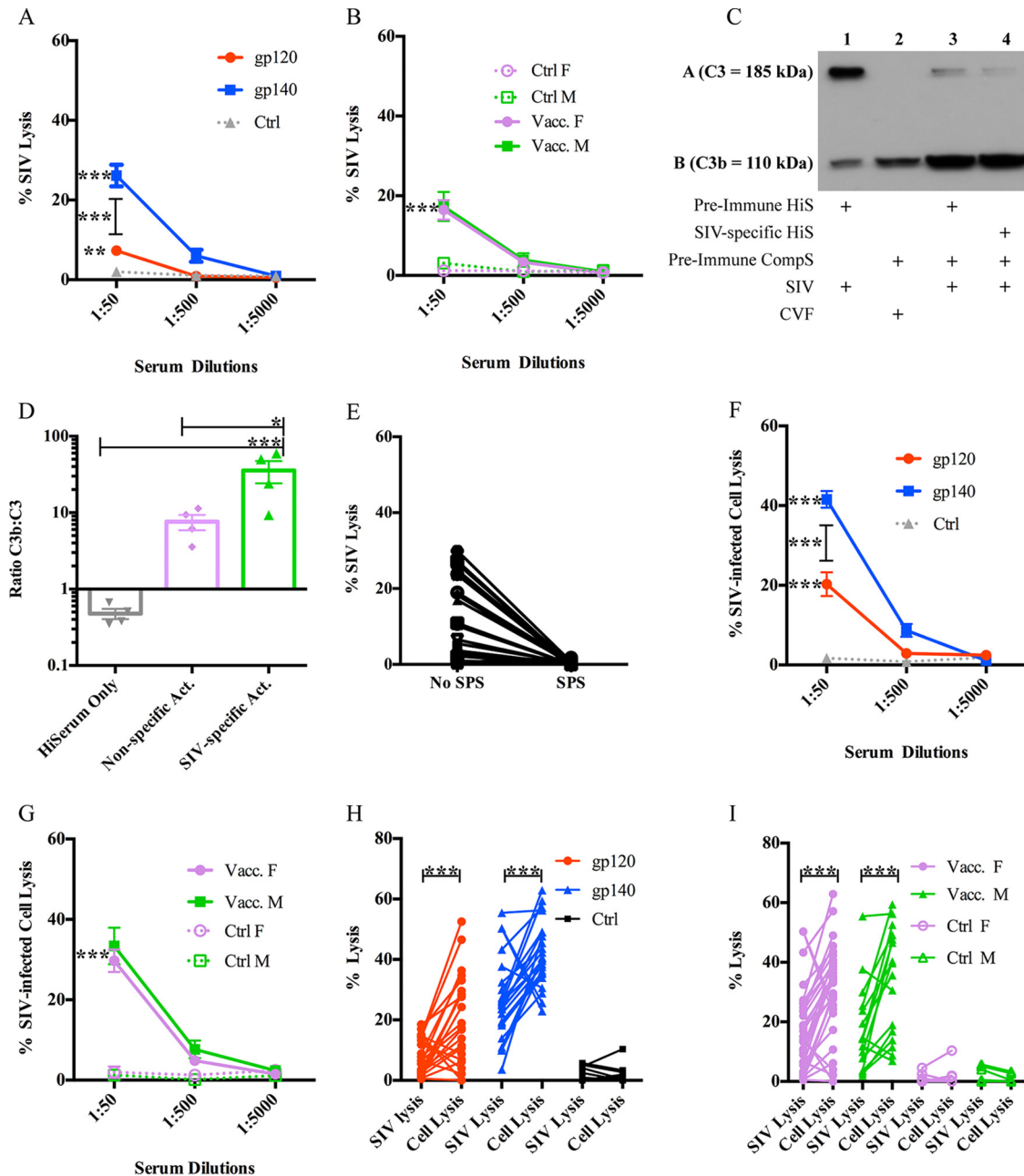
FIG 1 ADCML of SIV and SIV-infected cells. (A and B) Sera collected from all 60 macaques at week 57 were diluted as indicated and analyzed for ADCML of SIV. The average percent input SIV lysis is shown per dilution per animal cohort. The keys identify the animal cohorts immunized with gp120 or gp140, and error bars represent SEM. F, female; M, male. (C) Individual SIV ADCML assay well contents from 3 vaccinated macaques were analyzed for complement protein C3 activation via Western blotting; a representative blot from a single animal is shown. Row A represents C3 (185 kDa), and row B represents the C3 cleavage product C3b (110 kDa). +, components within each SIV ADCML assay well analyzed. (D) Western blot C3b band/C3 band density ratios were averaged per lane from 3 individual Western blots and are displayed in the histogram representing heat-inactivated serum only (lane 1 in panel C), nonspecific activity (Act.) (lane 3 in panel C), and SIV-specific activity (lane 4 in panel C). Error bars represent SEM. (E) Sera collected from 30 vaccinated macaques at week 57 were diluted 1:50 and analyzed for ADCML of SIV in the presence or absence of SPS. The symbols represent values from individual macaques. (F and G) Sera collected from all 60 macaques at week 57 were diluted as indicated and analyzed for ADCML of SIV-infected H9 cells. The average percent input SIV-infected cell lysis is shown per dilution per animal cohort. The keys identify the animal cohorts, and error bars represent SEM. (H and I) The ADCML of SIV and SIV-infected H9 cells was compared for all 60 animals. SIV and SIV-infected H9 cell lysis values are displayed per animal as two dots connected by a line. The keys identify the animal cohorts. Asterisks indicate significant differences (*, $P < 0.05$; **, $P < 0.01$; ***, $P < 0.001$). Abbreviations: HiS and HiSerum, heat-inactivated serum; CompS, complement serum; CVF, cobra venom factor.

samples containing nonspecific serum (Fig. 1C, lane 3, and D) can be attributed to antibody-independent mechanisms of complement activation, such as alternative pathway C3 tick-over (8, 9). As mentioned above, background complement activation resulted in less than 5% lysis of SIV, on average.

Second, we analyzed SIV ADCML in sera from 30 vaccinated macaques in the presence of the complement activation inhibitor sodium polyanetholesulfonate (SPS). SPS has been shown to inhibit complement activation by the classical and alternative pathways, presumably via adsorption of complement components (30). As expected, in the presence of SPS, SIV lysis was abrogated in all 30 assays using sera collected at week 57 (Fig. 1E) and also with week 53 sera (data not shown). Together, these data confirmed that the SIV lysis that we observed was indeed complement mediated.

Vaccine-induced antibodies mediate ADCML of SIV-infected cells. Next, we analyzed sera for ADCML of SIV-infected cells to determine if complement-mediated immunity has the potential to help control viral spread upon infection. For this purpose, human H9 cells infected with SIV_{mac251} were used in lieu of primary rPBMCs, as the culture could be maintained with a much higher percentage of infected cells, necessary for assay consistency and reliable detection of p27 release. ADCML of the infected cells was analyzed as described above using rhesus macaque sera collected at week 57. The same controls were performed as described above, along with one additional control. Uninfected H9 cells were incubated with the same macaque sera, and complement-mediated lysis was analyzed via a lactate dehydrogenase (LDH) release assay to control for nonspecific antibody-dependent or -independent macaque complement activation in the presence of human cells, which was subtracted as background from the SIV-specific ADCML of infected cell data. Again, sera from gp140-immunized animals lysed significantly more SIV-infected cells than sera from gp120-immunized animals ($P < 0.0001$) and mock-vaccinated control animals ($P < 0.0001$), lysing approximately 40% of input infected cells (Fig. 1F). Sera from gp120-immunized animals lysed approximately 20% of SIV-infected cells, which was significantly more than sera from mock-vaccinated animals as well (Fig. 1F; $P < 0.0001$). There were no significant differences in the percentage of SIV-infected cells lysed between sera from vaccinated male and female animals; when the animals were vaccinated, sera from both sexes were able to lyse significantly more SIV-infected cells (~30%) than sera from mock-vaccinated controls (Fig. 1G; $P < 0.0001$). Therefore, SIV-specific sera collected from vaccinated rhesus macaques were capable of lysing SIV-infected cells, indicating that vaccine-induced complement-mediated immunity also has the potential to suppress viral spread during SIV infection. A comparison of ADCML of SIV versus SIV-infected cells by sera from gp120- and gp140-immunized animals (Fig. 1H) and from males and females (Fig. 1I) showed that the percent lysis of SIV-infected cells was significantly greater than that of SIV virions (Fig. 1H, $P = 0.0006$ per comparison; Fig. 1I, $P = 0.001$ for males and $P = 0.0006$ for females). A potential explanation for this could be the fact that infected cells simply have a much higher number of viral envelope proteins on their surface than virions (virions have a low density of Env spikes), which could effectively decrease the threshold necessary for antibodies to cross-link and activate complement (31–34).

Limited impact of the complement regulatory protein CD59 on ADCML. There are a host of soluble and membrane-bound complement regulatory proteins that serve to control complement activation by inhibiting certain steps along the activation pathways (35). It is well-known that HIV can exploit some of these factors to escape complement-mediated attack, namely, CD46, CD55, CD59, and factor H (36–38). We purposefully did not inactivate or inhibit the majority of these factors during our experiments because their presence recapitulates the *in vivo* environment. However, one particular complement regulatory receptor, CD59, warranted further investigation as it specifically inhibits the formation of the membrane attack complex (MAC), the end stage of all three complement activation pathways that directly results in lysis of the

target. CD59 is a ubiquitously expressed glycosylphosphatidylinositol (GPI)-anchored cell surface receptor whose primary purpose is to protect healthy host cells from aberrant complement-mediated lysis. HIV acquires CD59 (as well as other complement regulatory cell surface proteins) when it buds from host cells, and it has been shown to protect HIV (and HIV-infected cells) from complement-mediated lysis (38–41). To assess the effects of CD59 in our system, we first stained rPBMCs collected from 25 naive, uninfected animals prior to vaccination with a CD59 antibody and analyzed the percentage of CD59$^+$ CD4$^+$ T cells, as they are the relevant host cell population that could contribute to SIV-associated CD59. Flow staining from one representative animal is shown in Fig. 2A to C. Approximately 85% of CD4$^+$ T cells collected from those prevaccinated animals expressed CD59 (Fig. 2D). The enzyme phosphoinositide phospholipase C (PIPLC) specifically cleaves GPI-anchored proteins, and when rPBMCs were incubated with PIPLC, less than 1% of CD4$^+$ T cells stained positive for CD59 (Fig. 2C). In these naive, uninfected rhesus macaques, there were no sex-specific differences in the percentage of CD59$^+$ CD4$^+$ T cells (Fig. 2D) or in the levels of CD59 expression, as indicated by the mean fluorescence intensity (MFI) values (data not shown). Moreover, in contrast to what has been reported in humans (41–43), we did not notice a decrease either in the percentage of CD59$^+$ CD4$^+$ T cells (Fig. 2D) or in the CD59 MFI (data not shown) following 8 weeks of SIV infection in the same macaques.

To determine the degree of ADCML inhibition imposed by the presence of CD59, we treated SIV with PIPLC and then analyzed SIV lysis using sera from 15 gp120-vaccinated macaques that lysed the least percentage of SIV in previous experiments. Surprisingly, we found that SIV lysis was only two times more efficient, on average, in the absence of CD59 both with week 57 sera (Fig. 2E, $P = 0.0027$) and with week 53 sera (data not shown). Moreover, CD59 removal did not rescue SIV lysis to levels comparable to the average CD59$^+$ SIV lysis efficiency that we observed in gp140-immunized animals. Again, we did not observe any significant sex differences in the fold enhancement of SIV ADCML following PIPLC treatment (data not shown), which corroborates our previous observation that males and females exhibit similar CD59 expression levels (Fig. 2D). These data suggest that CD59 might not provide the virus robust protection from ADCML; however, it cannot be ruled out that *in vitro*-propagated SIV does not efficiently acquire CD59 as it buds from rPBMCs. To explore this, we stained uninfected and SIV-infected H9 cells with a CD59 antibody and analyzed the percentage of CD59$^+$ live cells. Flow staining from one representative experiment is shown in Fig. 2F to H. Approximately 65% of uninfected and 42% of SIV-infected human H9 cells expressed CD59, on average (data not shown). This SIV infection-induced reduction in the percentage of human H9 cells that express CD59 was expected, as mentioned above, but we did not observe a significant difference in the CD59 MFI between uninfected and SIV-infected H9 cells (data not shown). Accordingly, despite the relatively robust CD59 expression on SIV-infected H9 cells, sera from vaccinated macaques were capable of lysing SIV-infected H9 cells (Fig. 1F and G). Consequently, we did not pursue further studies on CD59, as it did not drastically inhibit SIV or SIV-infected cell lysis in our system. While these data do not exclude the inhibitory impact of the other complement regulatory proteins that are likely active in our system, it does indicate that ADCML is indeed quantifiable *in vitro* despite their presence.

Sex differences associated with ADCML. After demonstrating that SIV ADCML could be reliably measured *in vitro*, we pursued our initial aim of determining whether this activity was associated with delayed SIV acquisition. We first examined the relationship between SIV lysis, mediated by week 57 sera collected 2 weeks before the first viral challenge, and the number of challenges required to infect each animal. Unexpectedly, we found that SIV lysis correlated with a reduced infection risk in vaccinated males, particularly in gp140-immunized males, but not in vaccinated females (Fig. 3A to F). As an overall significant delay of SIV acquisition was previously seen in vaccinated females but not males of this study (27), this result in a relatively small number of vaccinated male macaques suggested a modest effect on the rate of SIV infection and
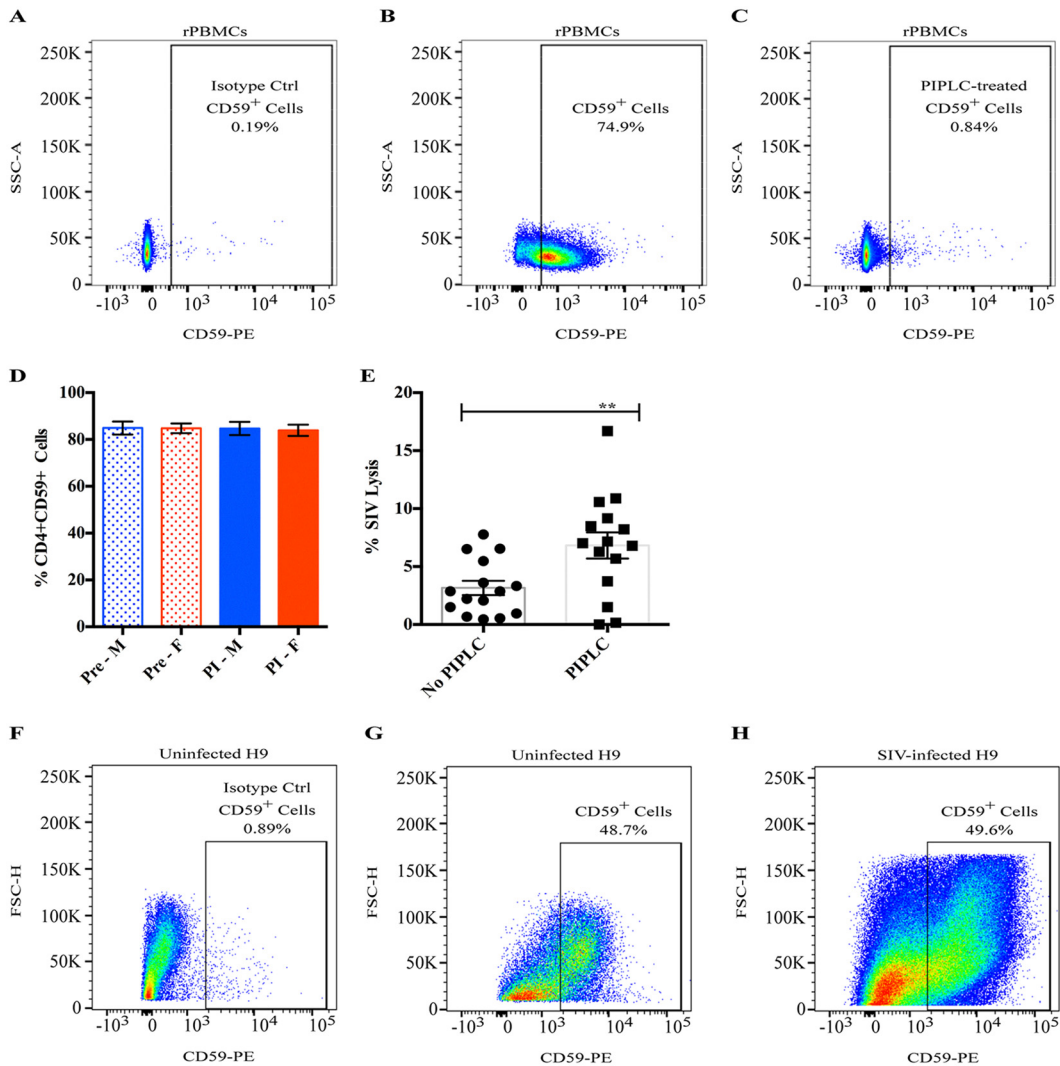
FIG 2 Cellular CD59 expression and inhibition of SIV lysis. (A to C) Naive, uninfected rPBMCs were evaluated for CD59 expression via flow cytometry: PE-isotype control staining (A), CD59-PE staining (B), and CD59-PE staining (C) of PIPLC-treated cells. The percentages of CD4$^+$ CD59$^+$ cells from one representative animal are shown. (D) rPBMCs were collected from 25 macaques prior to vaccination (Pre; dotted bars) and following 8 weeks of SIV infection (PI; solid bars), and CD4$^+$ T cells were evaluated for CD59 expression via flow cytometry. The average percentages of CD4$^+$ CD59$^+$ cells for males (blue) and females (red) at both time points are shown. Error bars represent SEM. (E) SIV was either treated with PIPLC or left untreated, and ADCML was assessed using sera collected from 15 gp120-immunized macaques at week 57. The symbols represent values from individual macaques, bars represent the average, and error bars represent SEM. Asterisks indicate a significant difference (**, $P <0.01$). (F to H) Human H9 cells were evaluated for CD59 expression via flow cytometry: PE-isotype control staining of uninfected H9 cells (F), CD59-PE staining of uninfected H9 cells (G), and CD59-PE staining of SIV-infected H9 cells (H). The percentages of live, CD59$^+$ cells from one representative experiment out of 3 individual experiments are shown.

will require verification in a future study. ADCML of SIV virions also impacted viral control, as an inverse association between SIV lysis and the peak viral load was observed in all gp140-immunized animals (Fig. 3G). In contrast to SIV lysis, we did not find any correlations between SIV-infected cell lysis and the infection rate or viral loads in any of the vaccinated animals. While ADCML did not influence the overall SIV acquisition rate in the vaccinated macaques, as reported earlier (27), the correlation between SIV lysis and the number of challenge exposures seen in vaccinated males suggested that this activity might differ between the sexes. Thus, we were prompted to further investigate sex differences in antibody titers, functions, and glycan profiles and their relationship to ADCML of SIV and SIV-infected cells.

Previously, we reported that week 53 sera, which were collected 2 weeks after the second protein boost, of vaccinated males had higher gp120-specific IgG titers (27)
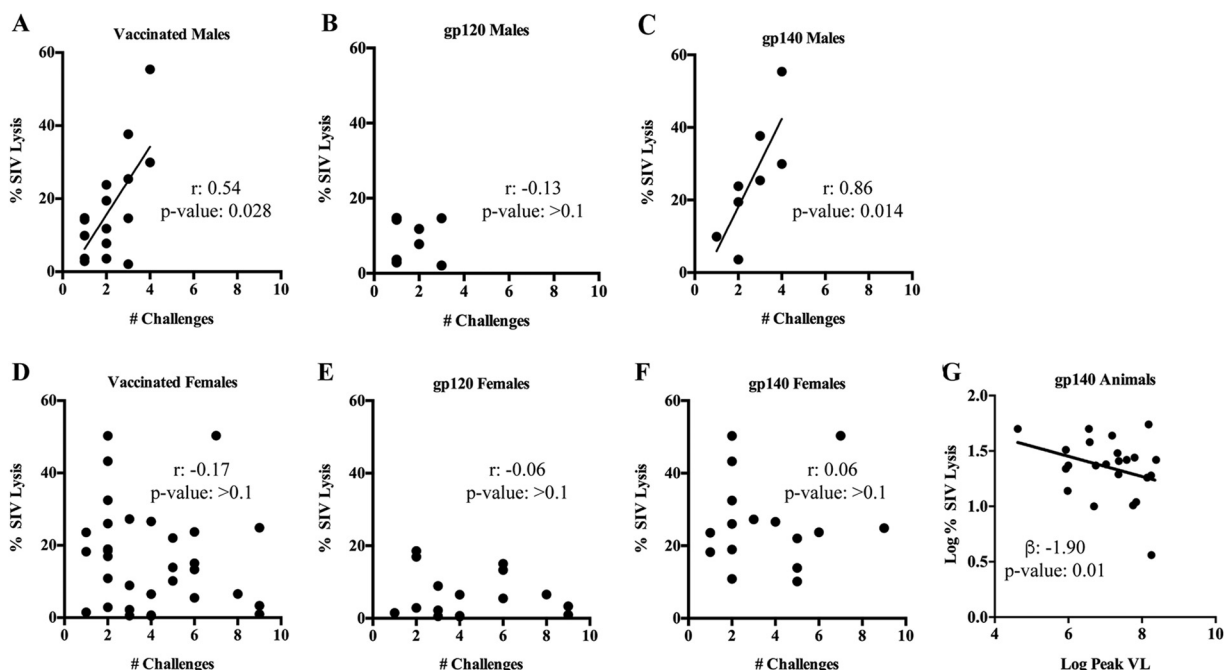
FIG 3 ADCML of SIV is associated with a reduced infection risk and the peak viral load only in certain animal cohorts. (A to F) Statistical correlations between ADCML of SIV and the number of challenges required to infect the animals are shown; the animal cohorts are displayed within each graph heading, and the symbols represent the values from individual macaques. Significant correlations, calculated using Spearman's rank correlation coefficient, are indicated by r, with P values being determined from the Jonckheere-Terpstra test. (G) An association between ADCML of SIV and the peak viral load (VL) in gp140-immunized animals is shown. The symbols represent values from individual macaques. The statistical significance of the association is indicated by the slope of the line (beta) and P value and was calculated using a linear regression model. Linear regression trend lines were added to significant correlations/associations for visual aid.

than sera of vaccinated females. Here, we examined sex differences in IgM titers since IgM antibodies are more potent activators of complement than antibodies of the IgG isotype (44). We found that vaccinated males had higher Env-specific (both gp120- and gp140-specific) IgM titers than vaccinated females (Fig. 4A [$P = 0.02$] and B [$P = 0.0017$]). Despite this, gp120-specific IgG and IgM titers correlated with SIV lysis only in vaccinated females (Fig. 4C and D). However, there were no significant correlations between gp140-specific antibodies of either isotype and SIV lysis in either sex. These results suggest that vaccine-induced gp120-specific antibodies in vaccinated males and females possess different functions and might indicate a difference in antibody functional synergies in males and females and/or that antibodies of alternative epitope specificity mediated ADCML of SIV in males. Additionally, while gp140-specific IgG titers correlated with SIV-infected cell lysis in all vaccinated animals (Fig. 4E), Env-specific IgM titers correlated with SIV-infected cell lysis only in vaccinated males (Fig. 4F and G). These results corroborate those presented above indicating that Env-specific IgM antibodies in males and females exhibit different functions. Although we previously reported that vaccinated females had higher percentages of gp120-specific IgG3 and gp140-specific IgG1, IgG2, and IgG3 than vaccinated males (28), here we observed no relationship of gp120/gp140-specific IgG subtypes with ADCML of either SIV or SIV-infected cells in the vaccinated animals.

Next, we assessed whether specific IgG antibody Fc-mediated functions, including ADCP and ADCC, correlated with ADCML. The ADCC and ADCP activities in the sera of the vaccinated macaques were previously reported; both sexes were shown to mediate Env-specific ADCP and ADCC with similar efficiencies, and no correlations between ADCP or ADCC activity and infection risk were found (27). Here, we found a correlation between gp120-targeted ADCP and ADCC activities in vaccinated males but not in females (Fig. 5A). Conversely, we found a correlation between SIV lysis and gp120-specific IgG (Fig. 4C) and gp120-targeted ADCP (Fig. 5B) in vaccinated females but not
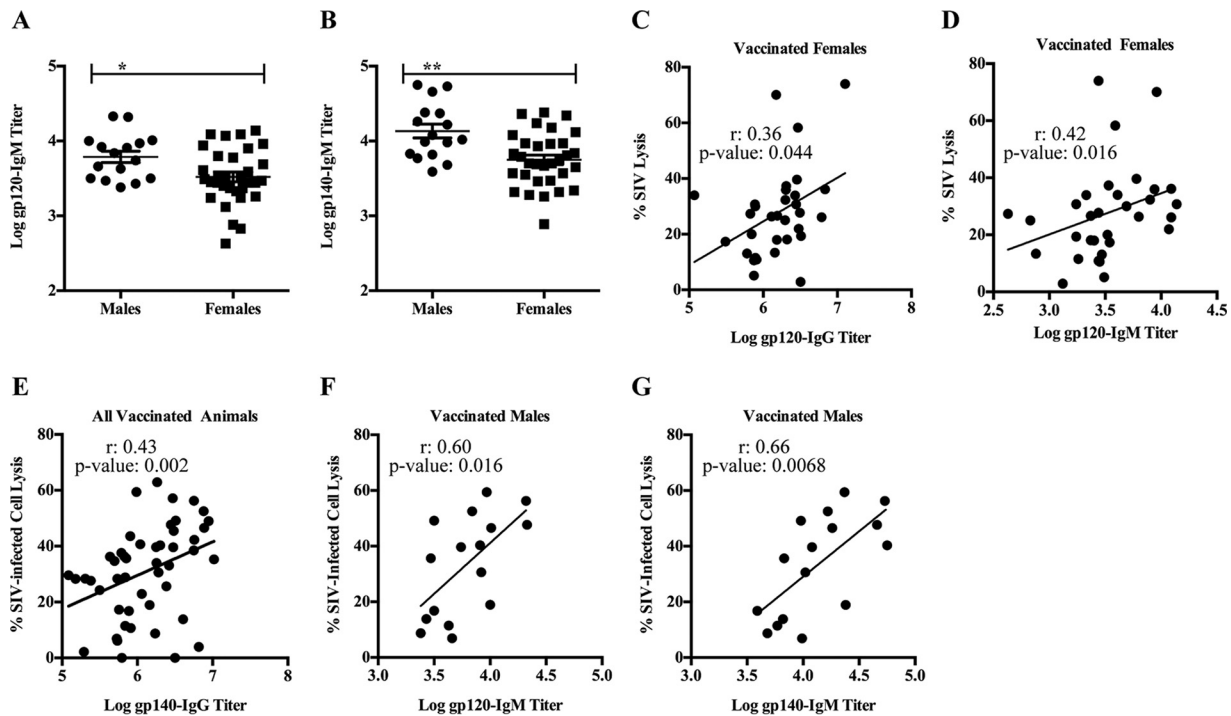
FIG 4 Env-specific IgG/IgM exhibit different ADCML capabilities in males and females. (A and B) Env-specific IgM binding titers were assessed in sera collected from all vaccinated macaques. gp120-specific (A) and gp140-specific (B) IgM binding titers are shown; error bars indicate SEM, and asterisks indicate significant differences between males and females (*, $P < 0.05$; **, $P < 0.01$). (C and D) Statistical correlations between ADCML of SIV and gp120-specific IgG binding titers (C) and IgM binding titers (D) are shown for all vaccinated females. (E to G) Statistical correlations between ADCML of SIV-infected H9 cells and gp140-specific IgG binding titers in all vaccinated animals (E) and gp120-specific (F) and gp140-specific (G) IgM binding titers in all vaccinated males are shown. The animal cohorts are displayed within each graph heading, and the symbols represent values from individual macaques. Significant correlations, calculated using Spearman's rank correlation coefficient, are indicated by r and P values and linear regression trend lines (added for visual aid).

in males. We also found a correlation between SIV-infected cell lysis, mediated by gp140-specific IgG antibodies in all animals (Fig. 4E) and gp140-targeted ADCC only in vaccinated males and not in females (Fig. 5C). These results revealed differential antibody Fc functional correlates among the vaccinees based on sex and together provide additional evidence that sex can have an effect on antibody Fc functionality. We hypothesized that these sex-based differences in antibody Fc functionality are potentially governed, at least partially, via the modulation of Fc glycosylation.
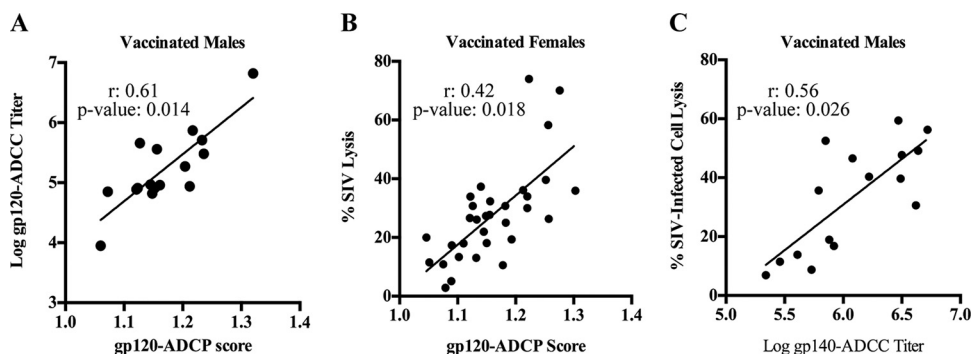

FIG 5 Sex differences in antibody Fc-mediated functionality. Statistical correlations between gp120-targeted ADCP and ADCC only in vaccinated males (A), ADCML of SIV and gp120-targeted ADCP only in vaccinated females (B), and ADCML of SIV-infected cells and gp140-targeted ADCC only in vaccinated males (C) are shown. The animal cohorts are displayed within each graph heading, and the symbols represent values from individual macaques. Significant correlations, calculated using Spearman's rank correlation coefficient and adjusted for immunization group, are indicated by r and P values and linear regression trend lines (added for visual aid).
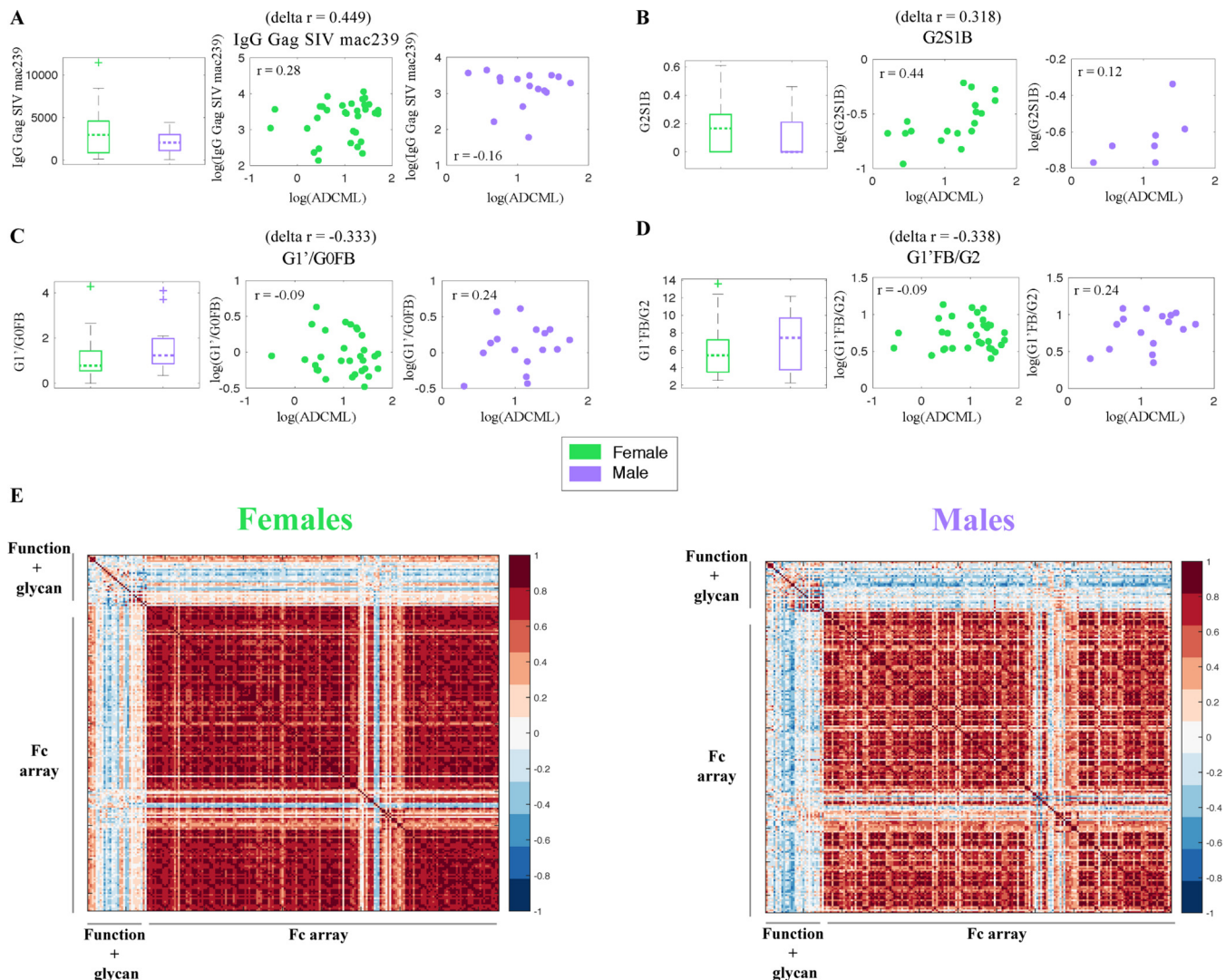
FIG 6 Systems serology approach to identify global sex differences in antibody profiles. (A to D) Box plots illustrate sex-specific levels, and scatter plots depict the sex-specific statistical correlations between SIV ACDML and IgG Gag SIV$_{mac239}$ (A), glycoform G2S1B (B), glycoform G1'/G0FB (C), and glycoform G1'FB/G2 (D). For panels B to D, the G in the glycoform name indicates galactosylation, S indicates sialylation, F indicates fucose, and B indicates a bisecting glycoform. The numbers that follow G and S indicate the number of galactose and sialic acid molecules. The symbols represent values from individual macaques, and correlation r and delta r values are displayed. (E) Sex-specific correlation heatmaps illustrating all pairwise Spearman correlations between the measured analytes (Fc effector functions, glycosylation profiles, and FcγR binding affinities).

To explore this hypothesis comprehensively, we utilized systems approaches to investigate sex-specific differences in a wide array of measured analytes in sera from vaccinated animals, including six Fc effector functions (ADCD, ADCC, ADCP, NK degranulation, NK production of gamma interferon and macrophage inflammatory protein 1β), 24 gp120-specific IgG glycans, and IgG titers, and Fcγ receptor (FcγR) binding capacity. We sought to identify analytes that differed by sex in terms of both their levels in females and males and their correlations with SIV lysis (Fig. 6). A global search across all the analytes measured using our systems serology platform revealed that females had higher IgG Gag titers (Fig. 6A) and increased gp120-specific IgG G2S1B glycoforms (Fig. 6B) that correspondingly correlated more strongly with ADCML (Fig. 6A and B) (in the glycoform names, G indicates galactosylation, S indicates sialylation, F indicates fucose, and B indicates a bisecting glycoform and the numbers that follow G and S indicate the number of galactose and sialic acid molecules). On the other hand, males had increased levels of gp120-specific IgG G1'/G0FB (Fig. 6C) and G1'FB/G2 (Fig. 6D) glycoforms that

correspondingly correlated more strongly with ADCML (Fig. 6C and D). Three of the four analytes that were different between males and females (from an unbiased global search), in terms of both the levels and the correlation with SIV ADCML, were gp120-specific IgG glycan substructures. These glycan-centric results corroborate the findings of previous studies highlighting sex-based biases in antibody glycosylation (45, 46) and indicate the potential mechanistic involvement of antibody glycosylation processes in the sex-specific variations in the correlations among IgG, ADCML, and the number of challenge exposures that we observed. Since we were able to tie the gender-specific differences in ADCML to specific glycan substructures, comprehensive profiling of the biochemical basis of differential glycosylation is likely to provide critical insights into different vaccine-induced immune response outcomes between the sexes.

Next, we explored whether the sex-specific variation was limited to a few key analytes (Fig. 6A to D) or whether the differences were more broadly pervasive. To this end, we examined all pairwise correlations between the measured responses. We found that there were striking differences in the overall correlation structure stratified by sex (Fig. 6E). These correlation profiles provide an unbiased global view of the coordination of the humoral immune responses in each sex. For example, there were stronger pairwise correlations within the measured antibody-dependent effector functions and associated glycosylation profiles in males than in females (Fig. 6E). In contrast, females exhibited stronger pairwise correlations between the measured biophysical responses (e.g., FcγR binding ability) than males (Fig. 6E). These results suggest that antibody glycosylation profiles and antibody effector functionality, i.e., qualitative aspects of the antibody response, were more tightly linked in males, while antibody FcγR binding affinities, i.e., rather quantitative aspects of the antibody response, were more tightly linked in females. Overall, our data imply that males and females respond differently to vaccine regimens and induce different flavors of antibody responses. Further comprehensive investigation of these responses will help us mechanistically elucidate how the same vaccine regimen can elicit antibodies with different properties and effector functions and, ultimately, different levels of protection in males and females.

DISCUSSION

Previously, we conducted an SIV vaccine efficacy study in rhesus macaques and found that females exhibited a significant delay in SIV acquisition compared to males due to enhanced local, mucosal B cell responses at the site of virus exposure (27). Subsequent studies revealed that several immune parameters developed differently in males and females, including Env-specific Tfh cells (29), Env-specific IgG3 levels, and Breg cells (28), with the last two influencing subsequent virus control. Here, to identify additional immune correlates of protection, we analyzed sera from the same vaccinated animals for their ability to activate complement and induce SIV and SIV-infected cell lysis. We found no sex differences in the induction of ADCML of either SIV or SIV-infected cells (Fig. 1). However, sera capable of mediating SIV lysis provided some protection from SIV acquisition in males but not in females (Fig. 3). It will be important to verify this result in future studies. Here, this modest effect was not sufficient to negate the overall difference in the SIV acquisition rate observed between the sexes, where a significant delay was seen in the females but not the males. It is likely that more than one immune parameter influences the acquisition rate. For example, the elevated Breg cell levels observed in the male macaques of this study were significantly correlated with peak viral loads, suggesting facilitation of SIV infection (28) and perhaps offsetting any benefit conveyed by a protective ADCML response. Additionally, we found that sera capable of mediating ADCC and ADCP, in addition to ADCML, as well as antibody glycosylation profiles differed between males and females (Fig. 4, 5, and 6). The differences between vaccinated males and females that we observed are in line with sex-based differences in basic immune biology that contribute to differential responses to vaccination.

The current study revealed a lack of uniformity in vaccine-induced antibody species

between animals of different sexes. Although correlative analyses do not reveal the mechanistic basis of biologic phenomena, they provide insight into biologic processes and thus guide further investigations. Here, we observed that gp120- and Gag-specific IgG correlated with ADCML of SIV only in females (Fig. 4C and 6A) but that gp140-specific IgG correlated with ADCML of SIV-infected cells in both sexes (Fig. 4E). Similarly, gp120-specific IgM correlated with ADCML of SIV only in females (Fig. 4D), while, in contrast, both gp120- and gp140-specific IgM correlated with ADCML of SIV-infected cells only in males (Fig. 4F and G). A possible explanation for the lack of correlation between the overall gp120-specific IgG titer, for example, and ADCML of SIV in males could be that the antibodies that mediate ADCML of SIV within the entire pool of Env-specific IgG in males recognize gp120 epitopes that were masked in the binding assay used to determine the titer of gp120-specific antibodies, thus preventing a correlation between the overall gp120-specific antibody titer and ADCML in males. In the absence of epitope mapping, this potential explanation cannot be validated, but the possibility of the phenomenon itself along with the correlation data obtained strengthen the notion that Env-specific antibodies capable of inducing ADCML of SIV and SIV-infected cells in males and females most likely recognized different Env epitopes. It is important to note that the extensive glycosylation of HIV/SIV Env is dependent upon the host cell and can dictate epitope exposure and availability for antibody binding. The SIV used for lysis experiments in this study was propagated in rPBMCs, while SIV-infected H9 cells were used for cell lysis experiments. Therefore, it is likely that Env glycosylation patterns were different between the two assay systems, providing different epitopes for recognition by Env-specific sera in vaccinated males and females. For example, gp120-specific IgM correlated with SIV lysis but not SIV-infected cell lysis in females, yet the opposite was true in males. This suggests that potential differences in the Env glycosylation patterns on the virus versus infected cells may have affected the exposure of gp120 epitopes such that gp120-specific IgM in females was precluded from inducing ADCML of infected cells but not virus, while gp120-specific IgM in males was precluded from inducing ADCML of virus but not infected cells. Together, these data suggest that gp120-specific IgM in females and males also recognized different epitopes. Sex-based differences in antibody epitope specificity could also reflect the effects of hormones on the development of antibody responses. Estrogen, for example, modulates B cell stimulation and survival (47) and can enhance humoral immunity in a dose-dependent manner (48).

Another explanation for the apparent lack of uniformity in vaccine-induced antibody functionality between the sexes could be differences in antibody Fc-region biology. Antibody Fc glycosylation can have profound effects on Fc-mediated functionality, including complement activation (49). All IgG antibodies are N-glycosylated in the C_H2 domain of the Fc portion, but terminal sugar residues can differ between fucose, galactose, bisecting *N*-acetylglucosamine, or sialic acid (49, 50). Importantly, the binding site for C1q, the complement recognition protein that triggers the classical pathway of complement activation, is also located in the C_H2 domain. In fact, agalactosylated or sialylated IgG antibodies are known to exhibit reduced C1q binding (49, 51), while galactosylated IgG antibodies exhibit increased binding (51). Examples of sex-specific differences in Fc glycosylation patterns do exist *in vivo* (52). For example, in healthy young adults the serum concentrations of agalactosylated IgG antibodies tend to be higher in males than in females (53). Therefore, the differences in the antibody species mediating ADCML in males compared to females could be the result of sex-specific Fc glycosylation patterns, which have also been documented in previous studies, affecting antibody functionality. One of the most dominant differences among antibodies is in glycosylation patterns; however, to our knowledge, this is the first study to examine such patterns following vaccination. Here, vaccine-induced gp120-specific IgG glycoforms that exhibited sex-specific differences both in abundance and in correlations with ADCML were G2S1B in females and G1′G0FB and G1′FB/G2 in males (Fig. 6A to D). Interestingly, the more abundant glycoforms in males that correlated strongly with ADCML were fucosylated, suggesting a testable hypothesis that a reduced inflamma-

tory response might be better associated with a reduced rate of infection in males (54, 55). Additionally, a global correlation analysis among Fc effector functions, glycan profiles, and FcγR binding affinities revealed that males exhibited stronger correlations between Fc effector functions and glycan profiles than females (Fig. 6E), suggesting that certain glycan signatures enhance Fc functionality more so in males than in females. Within a polyclonal pool of antibodies, IgG and other isotypes (such as IgM, which has 5 glycan sites that can be modified) likely work in concert to form immune complexes that may be exploited differently in males and females. IgG glycosylation can modulate Fc-mediated functions, namely, ADCC and ADCP, by affecting binding to FcγR that is expressed on effector cells, such as macrophages, dendritic cells, and natural killer cells. FcγR binding occurs in the C_H2 domain of the Fc portion of IgG, where glycosylation and C1q binding occur. In fact, C1q binding to IgG can affect FcγR engagement and subsequent effector function and vice versa (56, 57). Our global correlation analyses indicated a stronger correlation structure between gp120-specific IgG FcγR binding profiles in females than in males (Fig. 6E), indicating the possibility that vaccine-induced antibodies in females were better equipped to induce multiple Fc effector functions. Taken together, the data suggest that sex-based differences in Fc glycosylation profiles could have contributed to the differences in antibody functional correlates in males compared to females that we observed. Our findings motivate further exploration of global sex-specific differences in humoral immune responses. While in this study we focused on differential correlations, by sex, between ADCML and antibody-dependent effector functions, glycans, and Fc receptor binding, future studies may want to explore more thoroughly the relationships between other parameters of viral clearance that vary in a sex-specific manner and these Fc measurements. Additionally, the study here was conducted using SIV immunogens (SIV_{smH4}, SIV_{mac239}) and an SIV_{mac251} challenge. As SIV and HIV envelopes differ greatly in terms of antigenicity and susceptibility to antibody effector functions, it will be important to confirm the results presented here in a preclinical study in which HIV envelope immunogens are used along with a SHIV challenge and, ultimately, in a human trial.

Overall, our results suggest that vaccine-induced nonneutralizing antibodies capable of inducing complement-mediated immunity can greatly impact the immune response profile and potentially help steer vaccine outcomes. As such, modulating complement activation during vaccination through the use of adjuvants or complement-opsonized antigens should be explored as a means to enhance vaccine-induced immunity and protective efficacy. However, it will be important to determine the effect of modulating complement activation, in light of evidence that complement-opsonized HIV can exhibit enhanced infection through complement opsonin receptors expressed on important effector cells, such as follicular dendritic cells (13, 58–60). Our results also suggest that sex not only might affect vaccine-induced antibody Fc-mediated function but also might dictate immune requirements for protection from HIV infection. Therefore, we postulate that it will be important to consider sex differences in vaccine outcomes and susceptibility to HIV infection in order to design a highly effective HIV vaccine for all.

MATERIALS AND METHODS

Animals, immunizations, and challenge protocol. The 60 Indian rhesus macaques used in this study and the vaccine regimen and challenge protocol have been previously described (27). Briefly, macaques were housed, cared for, immunized, and challenged at Advanced Bioscience Laboratories, Inc. (ABL; Rockville, MD), or at Bioqual, Inc. (Rockville, MD). Following challenge, the macaques were maintained at the NIH Animal Facility. All animal care was in accordance with the guidelines of the Association for Assessment and Accreditation of Laboratory Animal Care and the recommendations of the *Guide for the Care and Use of Laboratory Animals* (61). Prior to initiation, all protocols and procedures were approved by the Institutional Animal Care and Use Committee of the respective facility. Macaques were primed at weeks 0 (intranasal and oral) and 12 (intratracheal) with three replication-competent adenovirus 5 host-range mutant (Ad5 hΔE3) recombinants separately encoding SIV_{smH4} *env* (gp140)/*rev*, SIV_{mac239} *gag*, and SIV_{mac239} *nef* lacking residues 1 to 13 (*nef*Δ_{1-13}). The animals were boosted intramuscularly at weeks 39 and 51 in MF59 adjuvant; the gp120 immunization group (16 females and 8 males) received soluble monomeric SIV_{mac239} gp120, and the gp140 immunization group (16 females and 8 males) received oligomeric SIV_{mac239} gp140. Both immunogens were produced in CHO cells (Novartis). Control macaques (7 females and 5 males) received the empty Ad5 hΔE3 vector and MF59 adjuvant. At

week 59, intrarectal, low-dose challenges with SIV$_{mac251}$ were initiated and repeated once per week (up to 9 weeks) until the animals became infected. Plasma viral loads were determined as described previously (27). Infection was determined by viral loads of ≥50 SIV RNA copies/ml. One female in the gp140-immunization group remained uninfected after 9 challenges.

Sample collection. Clotted blood samples were obtained from all 60 macaques prior to immunization, 2 weeks after the second protein boost (week 53), and 2 weeks prior to the first virus challenge (week 57). Clotted blood was centrifuged at 2,500 rpm for 15 min to separate the serum. Serum was aliquoted and stored at −80°C until use. EDTA blood samples obtained from 25 macaques prior to immunization and following 8 weeks of SIV infection were centrifuged over Ficoll gradients to separate the PBMCs. The PBMCs were washed, contaminating red blood cells were lysed, and PBMCs were stored in fetal bovine serum (FBS)–10% dimethyl sulfoxide in liquid nitrogen until use.

ADCML of SIV. Sera collected from the macaques at week 53 or at week 57 were individually thawed on ice and heat inactivated at 56°C for 1 h; this serum served as the source of SIV-specific antibodies in the assay. The heat-inactivated sera were diluted 50-fold, 500-fold, and 5,000-fold in gelatin Veronal buffer plus calcium and magnesium (GVB2^{++}; catalog number B102) from Complement Technology, Inc. (Tyler, TX), and 250 μl of each dilution was placed into duplicate wells of a 24-well plate. Stocks of SIV$_{mac251}$ grown in rPBMCs (250 ng/ml p27; 3.4 × 10^4 50% tissue culture infective doses/ml in rPBMCs), all originating from the same lot, were obtained from ABL and diluted 30-fold in GVB2^{++}, and 150 μl was added to each well. The plates were incubated at 37°C for 30 min. Autologous preimmune serum (collected prior to immunization) was diluted 10-fold, and 100 μl was added to each well; this serum served as the source of complement. The plates were incubated at 37°C for 1 h with agitation every 10 min. The contents of each well (100 μl) were analyzed in duplicate for p27 release using an SIV p27 enzyme-linked immunosorbent assay (ELISA) kit (catalog number 5450) from ABL according to the manufacturer's instructions, except that lysis buffer was not added, such that p27 was detectable only upon complement-mediated SIV lysis. The controls per animal included the following: (i) wells containing everything except autologous complement serum served as the negative control, (ii) wells containing preimmune heat-inactivated serum, complement serum, and SIV served as the control for non-SIV-specific complement activation, and (iii) wells containing everything except heat-inactivated serum served as the control for spontaneous, antibody-independent complement activation. Wells containing 150 μl of 30-fold-diluted SIV, 350 μl of GVB2^{++}, and 100 μl of p27 ELISA kit disruption buffer served as the positive control for 100% SIV lysis. Plate absorbance (Abs) values at 450 nm were obtained using a microplate spectrophotometer (BioTek PowerWave XS2). Percent SIV lysis was calculated per animal as follows: (i) blank well Abs values were subtracted from all sample well Abs values, (ii) p27 concentrations (in picograms per milliliter) were calculated based on the standard curve, which was run on the same plate, (iii) negative-control, non-SIV-specific control, and spontaneous complement control values were averaged and subtracted, and (iv) the values were divided by the average 100% lysis positive-control value and multiplied by 100. In the experiments which included the complement activation inhibitor SPS (catalog number 55963-78-5) from Sigma-Aldrich (St. Louis, MO), autologous preimmune complement serum was incubated with SPS at a final concentration of 2.5 mg/ml for 10 min on ice prior to use. In the experiments which included PIPLC-treated virus, SIV$_{mac251}$ was diluted 2-fold in GVB2^{++} to a final volume of 500 μl and incubated with 10 μl (equivalent to 1 unit) of PIPLC (catalog number P6466) from Thermo Fisher (Waltham, MA) at 37°C for 1 h prior to use.

ADCML of SIV-infected cells. SIV$_{mac251}$-infected human H9 cells were thawed and maintained in culture in RPMI medium supplemented with 10% FBS, glutamine, and penicillin-streptomycin. Uninfected human H9 cells were added to the culture every 3 days to maintain the culture infection. The percentage of SIV$_{mac251}$-infected H9 cells within the culture was periodically evaluated via intracellular staining with anti-SIV$_{mac251}$ p27 monoclonal antibody (clone KK64, catalog number 2321; NIH AIDS Reagent Program) (62) conjugated with Alexa Fluor 488 using the a Zenon Alexa Fluor 488 mouse IgG1 labeling kit (catalog number Z25002) from Thermo Fisher and flow cytometry. On average, the culture was maintained such that 45% of the human H9 cells used in these assays were infected with SIV$_{mac251}$. Sera collected from the macaques at week 57 were heat inactivated, diluted, and added to duplicate wells of a 24-well plate as described above. SIV$_{mac251}$-infected H9 cells (1 × 10^5) in 150 μl of GVB2^{++} were added to each well, and the plates were incubated at 37°C for 30 min. Autologous preimmune serum was diluted 5-fold, 100 μl was added to each well, and the plates were incubated at 37°C for 1 h with agitation every 10 min. The plates were centrifuged at 1,600 rpm for 8 min, and 100 μl of the supernatants was analyzed for p27 release as described above. Controls per animal were the same as those described above. Wells containing 1 × 10^5 SIV$_{mac251}$-infected H9 cells in 500 μl of GVB2^{++} and 100 μl of p27 ELISA kit disruption buffer served as the positive control for 100% SIV-infected cell lysis. Abs values were obtained, and SIV-infected cell lysis was calculated per animal as described above. Subsequently, another control value was subtracted as the background to control for nonspecific antibody-dependent or -independent macaque complement activation in the presence of human cells. To obtain this background control value, 1 × 10^5 uninfected H9 cells in 100 μl of GVB2^{++} were incubated with 100 μl of 50-fold-diluted heat-inactivated serum collected at week 57 (antibody-dependent species-specific complement activation control) or with 100 μl of GVB2^{++} (antibody-independent species-specific complement activation control) in a 96-well plate at 37°C for 30 min. Autologous preimmune serum was diluted 5-fold, 20 μl was added to each well, and the plates were incubated at 37°C for 1 h with agitation every 10 min. The plates were centrifuged at 250 × g for 4 min, and 50 μl of the supernatants was analyzed in duplicate for LDH release using a CytoTox 96 nonradioactive cytotoxicity kit (catalog number G1780) from Promega (Madison, WI) according to the manufacturer's instructions. Wells containing 1 × 10^5 uninfected H9 cells in 200 μl of GVB2^{++} and 20 μl of CytoTox kit lysis buffer served as the positive control for 100% uninfected cell lysis. Abs values at 490 nm were obtained as described above, and percent uninfected cell

lysis was calculated per animal as follows: (i) blank well Abs values were subtracted from all sample well Abs values, and (ii) the values were divided by the average 100% lysis positive-control value and multiplied by 100. The percentages of uninfected H9 cells that were lysed due to antibody-dependent and -independent species-specific complement activation were averaged and subtracted as background from the calculated SIV-infected cell lysis values.

Western blotting. The contents of SIV ADCML assay wells from 3 macaques, specifically, (i) the negative-control wells containing 50-fold-diluted heat-inactivated serum collected at week 53 and SIV$_{mac251}$, (ii) the non-SIV-specific complement activation control wells containing 50-fold-diluted heat-inactivated serum collected prior to immunization (the source of non-SIV-specific antibodies), SIV$_{mac251}$, and 10-fold-diluted preimmune serum (the source of complement), and (iii) the wells containing 50-fold diluted heat-inactivated serum collected at week 53 (the source of SIV-specific antibodies), SIV$_{mac251}$, and 10-fold-diluted preimmune serum (the source of complement), were analyzed for evidence of complement protein C3 cleavage via Western blotting to assess complement activation. A fourth sample was included as a positive control for complement activation and consisted of 10-fold-diluted preimmune serum (the source of complement) that had been incubated with cobra venom factor (catalog number A150) from Complement Technology, Inc., at a final concentration of 1 mg/ml for 30 min at 37°C. Twenty-five microliters (of the 500 μl in the well) from each sample was mixed with 25 μl of Laemmli buffer (catalog number 161-0737) from Bio-Rad (Hercules, CA) containing 5% 2-mercaptoethanol and incubated at 92°C for 10 min. Fifteen microliters was loaded per lane into a 4 to 20% Tris-glycine gradient gel (catalog number XP04205BOX) from Thermo Fisher. Protein bands were transferred onto a nitrocellulose membrane (catalog number IB3010-02) from Thermo Fisher using an iBlot dry blotting system from Thermo Fisher. The membrane was incubated in blocking buffer (Tris-buffered saline–Tween 20, 3% bovine serum albumin [BSA]) for 1 h. The proteins were probed using anti-C3/C3b/iC3b antibody (catalog number CL7636AP, clone 7C12) from CedarLane Labs (Burlington, NC) diluted 250-fold in blocking buffer for 18 h at 4°C. The membrane was washed 3 times in blocking buffer and incubated with peroxidase-conjugated goat anti-mouse IgG secondary antibody (catalog number 115-035-062) from The Jackson Laboratory (Sacramento, CA) diluted 2,000-fold in blocking buffer for 1 h at room temperature. The membrane was washed an additional 3 times, incubated with SuperSignal West Pico chemiluminescent substrate (catalog number 34080) from Thermo Fisher for 5 min at room temperature, and developed using film. Protein band sizes were determined based on the Novex Sharp prestained protein standard (catalog number LC5800) from Thermo Fisher. Band densities were determined using ImageJ (version 1.50i) software. Complement activation within each lane was calculated by dividing the C3b band (110-kDa) density by the C3 band (185-kDa) density.

CD59 staining and flow cytometry. rPBMCs (1.5×10^6) isolated from 25 macaques prior to vaccination and following 8 weeks of SIV$_{mac251}$ infection were stained with a LIVE/DEAD Fixable Aqua Dead cell stain kit (catalog number L34966) from Thermo Fisher and with the following antibodies: CD3-V450 (catalog number 560351, clone SP34-2) from BD Biosciences (San Jose, CA), CD4-Qdot-605 (catalog number CD4-Qdot-605, clone 19-Thy-5D7) from the Nonhuman Primate Reagent Resource, and CD59-phycoerythrin (PE) (catalog number GTX75576, clone MEM-43/5) from GeneTex (Irvine, CA) or the mouse IgG2b-PE isotype control (catalog number 555058, clone 27-35) from BD Biosciences. Stained cells were fixed with BD Cytofix fixation buffer (catalog number 554655) from BD Biosciences, and a minimum of 50,000 live, CD3$^+$ cells were acquired on a BD Biosciences LSR II flow cytometer and analyzed using FlowJo software (version 10.1). Cells were sequentially gated on singlets (forward scatter area [FSC-A]) versus forward scatter height [FSC-H], lymphocytes (side scatter area [SSC-A] versus FSC-A), live cells (Aqua dye negative), CD3$^+$/CD4$^+$ cells, and finally, CD59$^+$ cells. rPBMCs from 3 macaques were treated with PIPLC prior to antibody staining and flow cytometry analysis. For those experiments, 1.5×10^6 rPBMCs were resuspended in 500 μl of phosphate-buffered saline (PBS) and incubated with 10 μl (equivalent to 1 unit) of PIPLC at 37°C for 1 h prior to staining. On three separate occasions, 1.5×10^6 uninfected or SIV$_{mac251}$-infected human H9 cells were stained with a LIVE/DEAD Fixable Aqua Dead cell stain kit and with CD59-PE or a mouse IgG2b-PE isotype control. Stained cells were fixed and acquired as described above. Cells were sequentially gated on singlets (FSC-A versus FSC-H), live cells (Aqua dye negative), and finally, CD59$^+$ cells.

Serum antibody titers. Serum gp120- and gp140-specific IgG binding titers were assessed by ELISA and reported in a previous publication (27). Serum gp120- and gp140-specific IgG1, IgG2, and IgG3 binding titers were assessed by ELISA and reported in a previous publication (28). Serum gp120- and gp140-specific IgM binding titers were assessed by ELISA as follows: half-area plates were coated with either 50 μl of 1 μg/ml of SIV$_{mac239}$ gp140 or gp120 (Novartis) in carbonate-bicarbonate buffer (pH 9.6) for 18 h at 4°C. The plates were blocked with 100 μl of 1% BSA in Dulbecco-modified PBS (D-PBS) for 1 h at 37°C. Serum samples from week 53 were diluted 1:400 in D-PBS containing 1% BSA and 0.05% Tween 20. Fifty microliters of serial 2-fold dilutions of sera was incubated on the plate for 1 h at 37°C. The plates were washed 5 times, and primary goat anti-monkey IgM biotin-conjugated antibodies (catalog number 617-106-007) from Rockland Immunochemicals (Limerick, PA) were diluted 2,000-fold in D-PBS containing 1% BSA and 0.05% Tween 20 and incubated on the plate for 1 h at 37°C. The plates were washed 5 times, and secondary avidin D horseradish peroxidase-conjugated reagent (catalog number A-2004) from Vector Laboratories (Burlingame, CA) was diluted 1,000-fold in D-PBS containing 1% BSA and 0.05% Tween 20 and incubated on the plate for 1 h at 37°C. The plates were washed 5 times, and 50 μl of tetramethylbenzidine peroxidase substrate (catalog number 50-76-03) from KPL (Gaithersburg, MD) was incubated on the plate for 12 to 20 min at room temperature. Substrate development was stopped with the addition of 50 μl of 1 M phosphoric acid. Abs values at 450 nm were obtained as described above. The raw antibody titer was defined as the serum dilution

at which the Abs of the test serum was twice the mean Abs of the 12 blank wells, which was used to calculate the endpoint titers as previously described (63).

ADCC and ADCP. Serum nonneutralizing antibody activities ADCC and ADCP were assessed as previously described, and the 50% maximum killing ADCC titers and ADCP phagocytic scores were reported previously (27).

Systems analyses of correlations between the humoral immune response and ADCML. Frozen serum samples, collected from the macaques at week 53, were prepared and analyzed as previously described (64–66). We sought to identify gender-specific differences in coordination between ADCML and the measured analytes. An analyte (X) was said to be differentially coordinated by gender if it met the following stringent criteria: (i) the analyte had a significant difference, by gender, in magnitude. The difference in magnitude was considered significant if it met (a) an effect size threshold consisting of at least a 25% difference by gender and (b) a significance threshold consisting of the distributions of the analytes between male and female that were significantly different at a P value of <0.15 threshold (as measured by a one-sided Mann-Whitney U test, where values higher in females and higher in males were analyzed separately). We used a somewhat more permissive threshold of a P value of <0.15 rather than a more traditional P value of <0.05, as we required the analyte to satisfy several criteria, and we were looking to identify analytes that simultaneously satisfied all the criteria rather than ones that were very significantly different just in terms of magnitude. (ii) The analyte had a significant difference, by gender, in the Spearman correlation with ADCML. The difference in correlation was considered significant if it met (a) an effect size threshold consisting of an absolute value of the difference in Spearman correlation (i.e., delta correlation) between the two genders that was in the most extreme 10% of the whole distribution (across all analytes) of delta correlations and (b) a significance threshold consisting of the correlation that was significant in at least one gender at a Benjamini-Hochberg false discovery rate (FDR) of <0.2 threshold. The rationale behind using an FDR of <0.2 threshold rather than a more traditional 0.05 threshold is 2-fold. First, we used the more stringent multiple-testing correction-adjusted FDR (adjusting for testing the significance of Spearman correlations between ADCML and 209 analytes) instead of the less stringent unadjusted P values. Second, we were interested in identifying differences in correlations between genders rather than correlations that were very significant in a single gender. A significant difference in correlation can exist between genders, even if the correlation is moderately significant in one gender in one direction and weak/insignificant in the other gender in the opposite direction. These justify the use of a slightly more permissive FDR of <0.2 threshold. To examine global correlation profiles, we calculated pairwise Spearman correlations between all measured responses. The heatmaps illustrate these Spearman correlations, with the color corresponding to the value of the correlation (with the correspondence illustrated in the color bars). Statistical analyses were performed in Matlab.

Additional statistics. Data were analyzed using Prism software (v6.0; GraphPad Software). A P value of ≤ 0.05 was considered statistically significant. The following tests were used to evaluate statistical significance: the Wilcoxon rank sum test corrected for multiple comparisons by the method of Critchlow and Fligner (67) (Fig. 1A and F); multiple-comparisons one-way analysis of variance (ANOVA) (Fig. 1B and G); repeated-measures ANOVA (Fig. 1D); the Wilcoxon signed-rank test (Fig. 1H and I, and 2E); the nonparametric Spearman's rank correlation coefficient with the P value calculated using the Jonckheere-Terpstra test (Fig. 3A to F); linear regression analysis with SIV lysis, peak viral loads, and challenge number incorporated as terms in the model (Fig. 3G); the Mann-Whitney test (Fig. 4A and B); the nonparametric Spearman's rank correlation coefficient (Fig. 4C to G); and the nonparametric Spearman's rank correlation coefficient adjusted for immunization group (Fig. 5A to C).

REFERENCES

1. UNAIDS. 31 May 2016. Global AIDS update 2016. UNAIDS, Geneva, Switzerland. http://www.unaids.org/en/resources/documents/2016/Global-AIDS-update-2016. Accessed 1 May 2017.
2. Rerks-Ngarm S, Pitisuttithum P, Nitayaphan S, Kaewkungwal J, Chiu J, Paris R, Premsri N, Namwat C, de Souza M, Adams E, Benenson M, Gurunathan S, Tartaglia J, McNeil JG, Francis DP, Stablein D, Birx DL, Chunsuttiwat S, Khamboonruang C, Thongcharoen P, Robb ML, Michael NL, Kunasol P, Kim JH, MOPH-TAVEG Investigators. 2009. Vaccination with ALVAC and AIDSVAX to prevent HIV-1 infection in Thailand. N Engl J Med 361:2209–2220. https://doi.org/10.1056/NEJMoa0908492.

3. Corey L, Gilbert PB, Tomaras GD, Haynes BF, Pantaleo G, Fauci AS. 2015. Immune correlates of vaccine protection against HIV-1 acquisition. Sci Transl Med 7:310rv317. https://doi.org/10.1126/scitranslmed.aac7732.

4. Haynes BF, Gilbert PB, McElrath MJ, Zolla-Pazner S, Tomaras GD, Alam SM, Evans DT, Montefiori DC, Karnasuta C, Sutthent R, Liao HX, DeVico AL, Lewis GK, Williams C, Pinter A, Fong Y, Janes H, DeCamp A, Huang Y, Rao M, Billings E, Karasavvas N, Robb ML, Ngauy V, de Souza MS, Paris R, Ferrari G, Bailer RT, Soderberg KA, Andrews C, Berman PW, Frahm N, De Rosa SC, Alpert MD, Yates NL, Shen X, Koup RA, Pitisuttithum P, Kaewkungwal J, Nitayaphan S, Rerks-Ngarm S, Michael NL, Kim JH. 2012. Immune-correlates analysis of an HIV-1 vaccine efficacy trial. N Engl J Med 366:1275–1286. https://doi.org/10.1056/NEJMoa1113425.

5. Barouch DH, Liu J, Li H, Maxfield LF, Abbink P, Lynch DM, Iampietro MJ, SanMiguel A, Seaman MS, Ferrari G, Forthal DN, Ourmanov I, Hirsch VM, Carville A, Mansfield KG, Stablein D, Pau MG, Schuitemaker H, Sadoff JC, Billings EA, Rao M, Robb ML, Kim JH, Marovich MA, Goudsmit J, Michael NL. 2012. Vaccine protection against acquisition of neutralization-resistant SIV challenges in rhesus monkeys. Nature 482:89–93. https://doi.org/10.1038/nature10766.

6. Barouch DH, Alter G, Broge T, Linde C, Ackerman ME, Brown EP, Borducchi EN, Smith KM, Nkolola JP, Liu J, Shields J, Parenteau L, Whitney JB, Abbink P, Ng'ang'a DM, Seaman MS, Lavine CL, Perry JR, Li W, Colantonio AD, Lewis MG, Chen B, Wenschuh H, Reimer U, Piatak M, Lifson JD, Handley SA, Virgin HW, Koutsoukos M, Lorin C, Voss G, Weijtens M, Pau MG, Schuitemaker H. 2015. Protective efficacy of adenovirus/protein vaccines against SIV challenges in rhesus monkeys. Science 349: 320–324. https://doi.org/10.1126/science.aab3886.

7. Barouch DH, Stephenson KE, Borducchi EN, Smith K, Stanley K, McNally AG, Liu J, Abbink P, Maxfield LF, Seaman MS, Dugast AS, Alter G, Ferguson M, Li W, Earl PL, Moss B, Giorgi EE, Szinger JJ, Eller LA, Billings EA, Rao M, Tovanabutra S, Sanders-Buell E, Weijtens M, Pau MG, Schuitemaker H, Robb ML, Kim JH, Korber BT, Michael NL. 2013. Protective efficacy of a global HIV-1 mosaic vaccine against heterologous SHIV challenges in rhesus monkeys. Cell 155:531–539. https://doi.org/10.1016/j.cell.2013.09.061.

8. Merle NS, Church SE, Fremeaux-Bacchi V, Roumenina LT. 2015. Complement system part I—molecular mechanisms of activation and regulation. Front Immunol 6:262. https://doi.org/10.3389/fimmu.2015.00262.

9. Merle NS, Noe R, Halbwachs-Mecarelli L, Fremeaux-Bacchi V, Roumenina LT. 2015. Complement system part II: role in immunity. Front Immunol 6:257. https://doi.org/10.3389/fimmu.2015.00257.

10. Carroll MC. 1998. The role of complement and complement receptors in induction and regulation of immunity. Annu Rev Immunol 16:545–568. https://doi.org/10.1146/annurev.immunol.16.1.545.

11. Kacani L, Prodinger WM, Sprinzl GM, Schwendinger MG, Spruth M, Stoiber H, Dopper S, Steinhuber S, Steindl F, Dierich MP. 2000. Detachment of human immunodeficiency virus type 1 from germinal centers by blocking complement receptor type 2. J Virol 74:7997–8002. https://doi.org/10.1128/JVI.74.17.7997-8002.2000.

12. Posch W, Steger M, Knackmuss U, Blatzer M, Baldauf HM, Doppler W, White TE, Hortnagl P, Diaz-Griffero F, Lass-Florl C, Hackl H, Moris A, Keppler OT, Wilflingseder D. 2015. Complement-opsonized HIV-1 overcomes restriction in dendritic cells. PLoS Pathog 11:e1005005. https://doi.org/10.1371/journal.ppat.1005005.

13. Blue CE, Spiller OB, Blackbourn DJ. 2004. The relevance of complement to virus biology. Virology 319:176–184. https://doi.org/10.1016/j.virol.2003.11.029.

14. Israels J, Scherpbier HJ, Frakking FN, van de Wetering MD, Kremer LC, Kuijpers TW. 2012. Mannose-binding lectin and the risk of HIV transmission and disease progression in children: a systematic review. Pediatr Infect Dis J 31:1272–1278. https://doi.org/10.1097/INF.0b013e3182678bc4.

15. Ebenbichler CF, Thielens NM, Vornhagen R, Marschang P, Arlaud GJ, Dierich MP. 1991. Human immunodeficiency virus type 1 activates the classical pathway of complement by direct C1 binding through specific sites in the transmembrane glycoprotein gp41. J Exp Med 174: 1417–1424. https://doi.org/10.1084/jem.174.6.1417.

16. Susal C, Kirschfink M, Kropelin M, Daniel V, Opelz G. 1994. Complement activation by recombinant HIV-1 glycoprotein gp120. J Immunol 152: 6028–6034.

17. Okada N, Wu X, Okada H. 1997. Presence of IgM antibodies which sensitize HIV-1-infected cells to cytolysis by homologous complement in long-term survivors of HIV infection. Microbiol Immunol 41:331–336. https://doi.org/10.1111/j.1348-0421.1997.tb01209.x.

18. Aasa-Chapman MM, Holuigue S, Aubin K, Wong M, Jones NA, Cornforth D, Pellegrino P, Newton P, Williams I, Borrow P, McKnight A. 2005.

Detection of antibody-dependent complement-mediated inactivation of both autologous and heterologous virus in primary human immunodeficiency virus type 1 infection. J Virol 79:2823–2830. https://doi.org/10.1128/JVI.79.5.2823-2830.2005.

19. Haurum JS, Thiel S, Jones IM, Fischer PB, Laursen SB, Jensenius JC. 1993. Complement activation upon binding of mannan-binding protein to HIV envelope glycoproteins. AIDS 7:1307–1313. https://doi.org/10.1097/00002030-199310000-00002.

20. Senaldi G, Peakman M, McManus T, Davies ET, Tee DE, Vergani D. 1990. Activation of the complement system in human immunodeficiency virus infection: relevance of the classical pathway to pathogenesis and disease severity. J Infect Dis 162:1227–1232. https://doi.org/10.1093/infdis/162.6.1227.

21. Sullivan BL, Knopoff EJ, Saifuddin M, Takefman DM, Saarloos MN, Sha BE, Spear GT. 1996. Susceptibility of HIV-1 plasma virus to complement-mediated lysis. Evidence for a role in clearance of virus in vivo. J Immunol 157:1791–1798.

22. Gregersen JP, Mehdi S, Baur A, Hilfenhaus J. 1990. Antibody- and complement-mediated lysis of HIV-infected cells and inhibition of viral replication. J Med Virol 30:287–293. https://doi.org/10.1002/jmv.1890300411.

23. Spear GT, Takefman DM, Sullivan BL, Landay AL, Zolla-Pazner S. 1993. Complement activation by human monoclonal antibodies to human immunodeficiency virus. J Virol 67:53–59.

24. Huber M, Fischer M, Misselwitz B, Manrique A, Kuster H, Niederost B, Weber R, von Wyl V, Gunthard HF, Trkola A. 2006. Complement lysis activity in autologous plasma is associated with lower viral loads during the acute phase of HIV-1 infection. PLoS Med 3:e441. https://doi.org/10.1371/journal.pmed.0030441.

25. Page M, Quartey-Papafio R, Robinson M, Hassall M, Cranage M, Stott J, Almond N. 2014. Complement-mediated virus infectivity neutralisation by HLA antibodies is associated with sterilising immunity to SIV challenge in the macaque model for HIV/AIDS. PLoS One 9:e88735. https://doi.org/10.1371/journal.pone.0088735.

26. Perez LG, Martinez DR, deCamp AC, Pinter A, Berman PW, Francis D, Sinangil F, Lee C, Greene K, Gao H, Nitayaphan S, Rerks-Ngarm S, Kaewkungwal J, Pitisuttithum P, Tartaglia J, O'Connell RJ, Robb ML, Michael NL, Kim JH, Gilbert P, Montefiori DC. 2017. V1V2-specific complement activating serum IgG as a correlate of reduced HIV-1 infection risk in RV144. PLoS One 12:e0180720. https://doi.org/10.1371/journal.pone.0180720.

27. Tuero I, Mohanram V, Musich T, Miller L, Vargas-Inchaustegui DA, Demberg T, Venzon D, Kalisz I, Kalyanaraman VS, Pal R, Ferrari MG, LaBranche C, Montefiori DC, Rao M, Vaccari M, Franchini G, Barnett SW, Robert-Guroff M. 2015. Mucosal B cells are associated with delayed SIV acquisition in vaccinated female but not male rhesus macaques following SIVmac251 rectal challenge. PLoS Pathog 11:e1005101. https://doi.org/10.1371/journal.ppat.1005101.

28. Mohanram V, Demberg T, Musich T, Tuero I, Vargas-Inchaustegui DA, Miller-Novak L, Venzon D, Robert-Guroff M. 2016. B cell responses associated with vaccine-induced delayed SIVmac251 acquisition in female rhesus macaques. J Immunol 197:2316–2324. https://doi.org/10.4049/jimmunol.1600544.

29. Vargas-Inchaustegui DA, Demers A, Shaw JM, Kang G, Ball D, Tuero I, Musich T, Mohanram V, Demberg T, Karpova TS, Li Q, Robert-Guroff M. 2016. Vaccine induction of lymph node-resident simian immunodeficiency virus Env-specific T follicular helper cells in rhesus macaques. J Immunol 196:1700–1710. https://doi.org/10.4049/jimmunol.1502137.

30. Palarasah Y, Skjoedt MO, Vitved L, Andersen TE, Skjoedt K, Koch C. 2010. Sodium polyanethole sulfonate as an inhibitor of activation of complement function in blood culture systems. J Clin Microbiol 48:908–914. https://doi.org/10.1128/JCM.01985-09.

31. Yang X, Kurteva S, Ren X, Lee S, Sodroski J. 2005. Stoichiometry of envelope glycoprotein trimers in the entry of human immunodeficiency virus type 1. J Virol 79:12132–12147. https://doi.org/10.1128/JVI.79.19.12132-12147.2005.

32. Zhu P, Liu J, Bess J, Jr, Chertova E, Lifson JD, Grise H, Ofek GA, Taylor KA, Roux KH. 2006. Distribution and three-dimensional structure of AIDS virus envelope spikes. Nature 441:847–852. https://doi.org/10.1038/nature04817.

33. Diebolder CAB, Beurskens FJ, de Jong RN, Koning RI, Strumane K, Lindorfer MA, Voorhorst M, Ugurlar D, Rosati S, Heck AJ, van de Winkel JG, Wilson IA, Koster AJ, Taylor RP, Saphire EO, Burton DR, Schuurman J, Gros P, Parren PW. 2014. Complement is activated by IgG hexamers

assembled at the cell surface. Science 343:1260–1263. https://doi.org/10.1126/science.1248943.

34. Schiller J, Chackerian B. 2014. Why HIV virions have low numbers of envelope spikes: implications for vaccine development. PLoS Pathog 10:e1004254. https://doi.org/10.1371/journal.ppat.1004254.

35. Bajic G, Degn SE, Thiel S, Andersen GR. 2015. Complement activation, regulation, and molecular basis for complement-related diseases. EMBO J 34:2735–2757. https://doi.org/10.15252/embj.201591881.

36. Montefiori DC, Cornell RJ, Zhou JY, Zhou JT, Hirsch VM, Johnson PR. 1994. Complement control proteins, CD46, CD55, and CD59, as common surface constituents of human and simian immunodeficiency viruses and possible targets for vaccine protection. Virology 205:82–92. https://doi.org/10.1006/viro.1994.1622.

37. Stoiber H, Pinter C, Siccardi AG, Clivio A, Dierich MP. 1996. Efficient destruction of human immunodeficiency virus in human serum by inhibiting the protective action of complement factor H and decay accelerating factor (DAF, CD55) J Exp Med 183:307–310.

38. Saifuddin M, Hedayati T, Atkinson JP, Holguin MH, Parker CJ, Spear GT. 1997. Human immunodeficiency virus type 1 incorporates both glycosyl phosphatidylinositol-anchored CD55 and CD59 and integral membrane CD46 at levels that protect from complement-mediated destruction. J Gen Virol 78(Pt 8):1907–1911.

39. Saifuddin M, Ghassemi M, Patki C, Parker CJ, Spear GT. 1994. Host cell components affect the sensitivity of HIV type 1 to complement-mediated virolysis. AIDS Res Hum Retroviruses 10:829–837. https://doi.org/10.1089/aid.1994.10.829.

40. Saifuddin MP, Parker CJ, Peeples ME, Gorny MK, Zolla-Pazner S, Ghassemi M, Rooney IA, Atkinson JP, Spear GT. 1995. Role of virion-associated glycosylphosphatidylinositol-linked proteins CD55 and CD59 in complement resistance of cell line-derived and primary isolates of HIV-1. J Exp Med 182:501–509. https://doi.org/10.1084/jem.182.2.501.

41. Schmitz J, Zimmer JP, Kluxen B, Aries S, Bogel M, Gigli I, Schmitz H. 1995. Antibody-dependent complement-mediated cytotoxicity in sera from patients with HIV-1 infection is controlled by CD55 and CD59. J Clin Invest 96:1520–1526. https://doi.org/10.1172/JCI118190.

42. Weiss L, Okada N, Haeffner-Cavaillon N, Hattori T, Faucher C, Kazatchkine MD, Okada H. 1992. Decreased expression of the membrane inhibitor of complement-mediated cytolysis CD59 on T-lymphocytes of HIV-infected patients. AIDS 6:379–385. https://doi.org/10.1097/00002030-199204000-00004.

43. Terpos E, Sarantopoulos A, Kouramba A, Katsarou O, Stavropoulos J, Masouridi S, Karafoulidou A, Meletis J. 2008. Reduction of CD55 and/or CD59 in red blood cells of patients with HIV infection. Med Sci Monit 14:CR276–CR280.

44. Wagner E, Frank MM. 2010. Therapeutic potential of complement modulation. Nat Rev Drug Discov 9:43–56. https://doi.org/10.1038/nrd3011.

45. Ercan A, Kohrt WM, Cui J, Deane KD, Pezer M, Yu EW, Hausmann JS, Campbell H, Kaiser UB, Rudd PM, Lauc G, Wilson JF, Finkelstein JS, Nigrovic PA. 2017. Estrogens regulate glycosylation of IgG in women and men. JCI Insight 2:e89703. https://doi.org/10.1172/jci.insight.89703.

46. Pucic M, Knezevic A, Vidic J, Adamczyk B, Novokmet M, Polasek O, Gornik O, Supraha-Goreta S, Wormald MR, Redzic I, Campbell H, Wright A, Hastie ND, Wilson JF, Rudan I, Wuhrer M, Rudd PM, Josic D, Lauc G. 2011. High throughput isolation and glycosylation analysis of IgG—variability and heritability of the IgG glycome in three isolated human populations. Mol Cell Proteomics 10:M111.010090. https://doi.org/10.1074/mcp.M111.010090.

47. Drehmer MN, Suterio DG, Muniz YC, de Souza IR, Lofgren SE. 2016. BAFF expression is modulated by female hormones in human immune cells. Biochem Genet 54:722–730. https://doi.org/10.1007/s10528-016-9752-y.

48. Gianella S, Tsibris A, Barr L, Godfrey C. 2016. Barriers to a cure for HIV in women. J Int AIDS Soc 19:20706. https://doi.org/10.7448/IAS.19.1.20706.

49. Karsten CM, Kohl J. 2012. The immunoglobulin, IgG Fc receptor and complement triangle in autoimmune diseases. Immunobiology 217:1067–1079. https://doi.org/10.1016/j.imbio.2012.07.015.

50. Raju TS. 2008. Terminal sugars of Fc glycans influence antibody effector functions of IgGs. Curr Opin Immunol 20:471–478. https://doi.org/10.1016/j.coi.2008.06.007.

51. Quast I, Keller CW, Maurer MA, Giddens JP, Tackenberg B, Wang L, Munz C, Nimmerjahn F, Dalakas MC, Lunemann JD. 2015. Sialylation of IgG Fc domain impairs complement-dependent cytotoxicity. J Clin Invest 125:4160–4170. https://doi.org/10.1172/JCI82695.

52. Chen G, Wang Y, Qiu L, Qin X, Liu H, Wang X, Wang Y, Song G, Li F, Guo Y, Li F, Guo S, Li Z. 2012. Human IgG Fc-glycosylation profiling reveals associations with age, sex, female sex hormones and thyroid cancer. J Proteomics 75:2824–2834. https://doi.org/10.1016/j.jprot.2012.02.001.

53. Yamada E, Tsukamoto Y, Sasaki R, Yagyu K, Takahashi N. 1997. Structural changes of immunoglobulin G oligosaccharides with age in healthy human serum. Glycoconj J 14:401–405. https://doi.org/10.1023/A:1018582930906.

54. Jefferis R. 2009. Glycosylation as a strategy to improve antibody-based therapeutics. Nat Rev Drug Discov 8:226–234. https://doi.org/10.1038/nrd2804.

55. Shade K-T, Anthony RM. 2013. Antibody glycosylation and inflammation. Antibodies 2:392–414. https://doi.org/10.3390/antib2030392.

56. Idusogie EE, Wong PY, Presta LG, Gazzano-Santoro H, Totpal K, Ultsch M, Mulkerrin MG. 2001. Engineered antibodies with increased activity to recruit complement. J Immunol 166:2571–2575. https://doi.org/10.4049/jimmunol.166.4.2571.

57. Mehlhop E, Nelson S, Jost CA, Gorlatov S, Johnson S, Fremont DH, Diamond MS, Pierson TC. 2009. Complement protein C1q reduces the stoichiometric threshold for antibody-mediated neutralization of West Nile virus. Cell Host Microbe 6:381–391. https://doi.org/10.1016/j.chom.2009.09.003.

58. Montefiori DC. 1995. New insights into the role of host cell proteins in antiviral vaccine protection. AIDS Res Hum Retroviruses 11:1429–1431. https://doi.org/10.1089/aid.1995.11.1429.

59. Willey S, Aasa-Chapman MM, O'Farrell S, Pellegrino P, Williams I, Weiss RA, Neil SJ. 2011. Extensive complement-dependent enhancement of HIV-1 by autologous non-neutralising antibodies at early stages of infection. Retrovirology 8:16. https://doi.org/10.1186/1742-4690-8-16.

60. Ellegard R, Crisci E, Burgener A, Sjowall C, Birse K, Westmacott G, Hinkula J, Lifson JD, Larsson M. 2014. Complement opsonization of HIV-1 results in decreased antiviral and inflammatory responses in immature dendritic cells via CR3. J Immunol 193:4590–4601. https://doi.org/10.4049/jimmunol.1401781.

61. National Research Council. 2011. Guide for the care and use of laboratory animals, 8th ed. National Academies Press, Washington, DC.

62. Kent KA, Gritz L, Stallard G, Cranage MP, Collignon C, Thiriart C, Corcoran T, Silvera P, Stott EJ. 1991. Production and of monoclonal antibodies to simian immunodeficiency virus envelope glycoproteins. AIDS 5:829–836. https://doi.org/10.1097/00002030-199107000-00006.

63. Frey A, Di Canzio J, Zurakowski D. 1998. A statistically defined endpoint titer determination method for immunoassays. J Immunol Methods 221:35–41. https://doi.org/10.1016/S0022-1759(98)00170-7.

64. Brown EP, Dowell KG, Boesch AW, Normandin E, Mahan AE, Chu T, Barouch DH, Bailey-Kellogg C, Alter G, Ackerman ME. 2017. Multiplexed Fc array for evaluation of antigen-specific antibody effector profiles. J Immunol Methods 443:33–44. https://doi.org/10.1016/j.jim.2017.01.010.

65. Chung AW, Kumar MP, Arnold KB, Yu WH, Schoen MK, Dunphy LJ, Suscovich TJ, Frahm N, Linde C, Mahan AE, Hoffner M, Streeck H, Ackerman ME, McElrath MJ, Schuitemaker H, Pau MG, Baden LR, Kim JH, Michael NL, Barouch DH, Lauffenburger DA, Alter G. 2015. Dissecting polyclonal vaccine-induced humoral immunity against HIV using systems serology. Cell 163:988–998. https://doi.org/10.1016/j.cell.2015.10.027.

66. Lu LL, Chung AW, Rosebrock TR, Ghebremichael M, Yu WH, Grace PS, Schoen MK, Tafesse F, Martin C, Leung V, Mahan AE, Sips M, Kumar MP, Tedesco J, Robinson H, Tkachenko E, Draghi M, Freedberg KJ, Streeck H, Suscovich TJ, Lauffenburger DA, Restrepo BI, Day C, Fortune SM, Alter G. 2016. A functional role for antibodies in tuberculosis. Cell 167:433–443.e414. https://doi.org/10.1016/j.cell.2016.08.072.

67. Critchlow ED, AM Fligner. 1991. On distribution-free multiple comparisons in the one-way analysis of variance. Commun Stat Theory Methods 20:127–139. https://doi.org/10.1080/03610929108830487.